Solid State Sciences 75 (2018) 71–76

Contents lists available at ScienceDirect

Solid State Sciences

journal homepage: www.elsevier.com/locate/ssscie

Pencil sketch graphene films as solid lubricant on steel surface: Observation of transition to grapehene/amorphous carbon

Bin Zhang [a, b, *], Yong Xue [a, c], Kaixong Gao [a, d], Li Qiang [a, d], Yuanlie Yu [a], Zhenbin Gong [a, d], Aimin Liang [a], Junyan Zhang [a], Baoping Yang [c]

[a] R&D Center of Lubricating and Protecting Materials, Key Laboratory of Solid Lubrication, Lanzhou Institute of Chemical Physics, Chinese Academy of Sciences, Lanzhou 730000, PR China
[b] Lawrence Berkeley National Laboratory, 1 Cyclotron Road, Berkeley, CA 94720, USA
[c] School of Petrochemical Technology, Lanzhou University of Technology, Lanzhou 730050, PR China
[d] University of Chinese Academy of Sciences, Beijing 100049, PR China

ARTICLE INFO

Article history:
Received 25 August 2017
Received in revised form
12 October 2017
Accepted 13 October 2017
Available online 16 October 2017

Keywords:
Graphene
Amorphous carbon
Lubricant
Low friction
Low wear

ABSTRACT

During recent years, graphene as a solid lubrication material have been thoroughly studied under nano or micro scales, but rarely reported at industrial conditions. In present work, graphene films as solid lubricant were prepared on the surface of 201 stainless steel substrates by pencil sketch. And then the friction tests from 5 to 65 N were carried out via a homemade tribo-tester and used GCr15 balls (ø = 5 mm) as friction pairs. Not surprisingly, graphene films cannot bear the loads beyond 5 N, but interestingly, via gradually increasing the loads, graphene films show prominent load performance and steady state of friction coefficients at about 0.12 while the loads varied from 5 to 65 N. Compared with bare steel, the coefficient of graphene films reduced by about 80%, and the wear volume reduced to 1/28 when variable load (from 5 N to 30 N) were applied. Raman spectra shown that the structure of graphene had been changing into diamond-like carbon films with graphene distributed inside, which was confirmed by HRTEM that graphenes were coming with amorphous carbon. Considering the roughness of steel wafers (170 nm), one can speculate that, with graphene films' protection, the steel has no abrasion but plastic deformation instead. It is concluded that the shearing force induced the film densification via sp^2 to sp^3 changing that enforced cross-linking. This cross-linking carbon matrix was responsible for high load bearing and the graphene exfoliated into graphene under shearing force contribute to low steady-state friction. Benefiting from sketch, one can get a lubrication film on any substrates with complex topography, our results shed light on the growth of graphene films for industrial use.

1. Introduction

Precisely, friction and wear happen between surfaces and interfaces in relative motions. They are usually viewed as inevitable and irreversible process when the machines are running, which is regarded as one of three main forms (wear, corrosion and breakage) of the materials failure with energy dissipation (friction) and material deterioration (wear) [1]. This process is accompanying by the losses of material surface and change of parts size, which will finally affect the life of the machines directly. Thus, the friction and wear properties of materials are crucial for their applications. Control friction, reduce wear and improve lubrication are urgent demands to solve scientific and engineering problems. In most cases, lubrication plays a significant role in reduce energy consumption and prolong the life span of machines [2].

Two-dimensional materials, like graphite, graphene, molybdenum disulfide and hexagonal boron nitride nanosheets are believed prominent lubricious materials due to its low shear force between layered structures [3–10]. Some of reports proved that these layer stacked films showed supelubricity properties sometimes, but most of reports showed that high friction coefficient in the scope of 0.01–0.2 [3–14]. Among them, grahene and multilayer-graphene are most prominent ones because of weak van der waals interaction which is 52 ± 5 meV per atom [15–19]. This unique property

* Corresponding author. Lawrence Berkeley National Laboratory, 1 Cyclotron Road, Berkeley, CA 94720, USA.
E-mail address: bzhang@licp.cas.cn (B. Zhang).

https://doi.org/10.1016/j.solidstatesciences.2017.10.005
1293-2558/

makes graphene layers can slide freely over another. Since using graphene as a solid lubrication has been studied for centuries. Usually, graphene shows high friction in vaccum due to mill into dust but low friction in oxygen, water vapor, and air environments, owing to the absorption of molecules which significantly lowers the cleavage energy [20,21]. Interestingly, Kumar showed that graphene friction properties strong correlated with atmosphere [22]. In Ar atmosphere, super-low friction is appear. However, in oxygen or nitrogen, high friction is prominent due to presence more dagling bonding [22]. Recent study proved that super-lubricity could achive due to the incommensurate contact in nanoscale [3–5,7,16.23]. But friction properties are more complicate in macroscale because the frciton depends on the orietation of graphene between interface [23]. Friction coefficients, tested on paralle and pendicular, show a opposite trend to the friction because that paralled graphene has lower dangling bonds than that of which pendicular to substrates that holds a more high adhensive effects [24]. As a result, the super-lubricity property always reffers that phenomeno between two paralle graphene or graphite [3–5]. In the knowlege of the authors, graphene as a luburication is used for years and some of articles have discussed the lubricity under appearance based or at nanoscale, but it is obviously very difference from industrial sacles that high load might destroy layered stacks. Thus, how graphene reduces friction and wear remains uncertain under high loads, In this article, our goals are aming to the possibility of graphene films using under industrial condition and to reveal the possible mechanism for lubrication and anti-wear under high contact pressure.

Herein, inspired by pencil sketch which is employed by many other artists, for example, portrait of Adolpyh Von Menzel, we successfully prepared graphene films on the surfaces of stainless steel substrates using a 2B pencil. The preparation process is shown in Fig. 1, which is a way with flexible, environment friendly, efficient and economy. Then, the tribological performances and the structural evolution of the resulted films were investigated by using the variable load process, Raman spectroscope and high-resolution transmission electron microscopy (HRTEM), etc. The results indicate that the as-fabricated films possess excellent anti-friction and wear-resistance performances. In addition, based on the characterization results, possible mechanism for the enhanced anti-friction and wear-resistance properties is also proposed. The shearing force induced the film densification by promoting sp^2 to sp^3 changing which enforced cross-linking. This cross-linking carbon matrix was responsible for high load bearing. Moreover, the graphene exfoliated under shearing force contributes to the low stead-state friction.

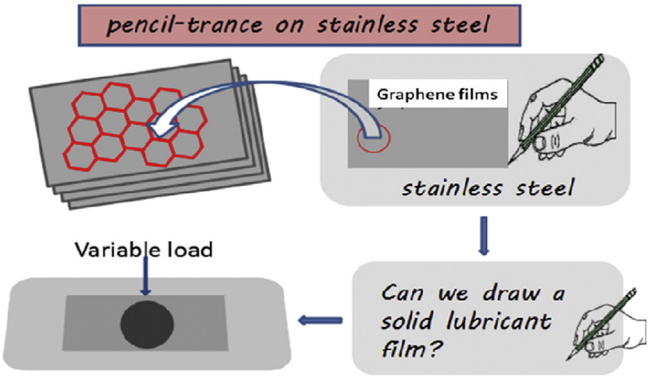

Fig. 1. A schematic representation of the pencil sketch process on stainless steel substrate.

2. Experimental section

Prior to preparation, all stainless steel wafers were cleaned by sonication for more than 30 min in ethanol solution in an ultrasonic bath to remove contaminants left from the sample preparation steps, and subsequently blown dry with N_2. After that, graphene films were obtained by pencil (2B) sketch on stainless steel wafers along the perpendicular to the direction of the texture of the wafer, parallel to the direction of reciprocation.

The tribological experiments of the graphene films were conducted on a multifunctional material surface performance tester with a ball on disk contact geometry at room temperature (25–28 °C) and relative humidity (RH) of 42–45% in ambient air. During this course we chosen GCr15 balls (ø = 5 mm) as the stationary upper counterparts. The friction tests were carried out along the sketch direction, namely, perpendicular to the direction of the texture of the wafer. Considering the binding force of the sketched films with the substrate is relatively weak. At the beginning applied a high load, as a result the films will be worn out soon. To avoid the films being worn instantaneously, which requires an ever-increasing load applied to form transfer films in the process of friction. In this research, we chosen 5 N as initial normal load for 15 min for the densification of the films, then increased the load to 10 N in every 10 min, until increased the load to 65 N. Other test parameters include sliding velocity (240 mm/min) and slide stroke (5 mm). The COF was calculated by the formula as COF= F/L, where F is the frictional force in N, L is the applied normal load in N. In order to avoid the randomness of experiment results and make it more convinced. All friction experiments were repeatedly performed for more than three times under the same conditions.

After friction tests, Raman spectroscope (LABRAM HR 800 at a

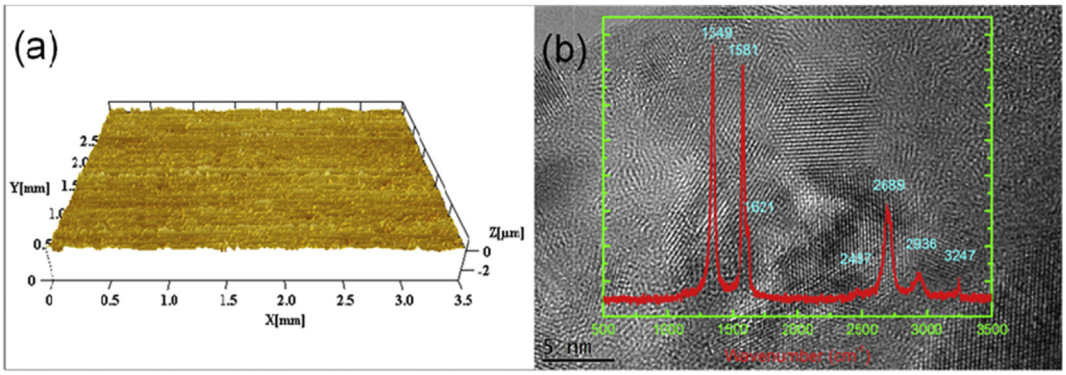

Fig. 2. (a) AFM image of 201 stainless steel and (b) HRTEM image of as-prepared films and corresponding Raman spectra (as inseted in).

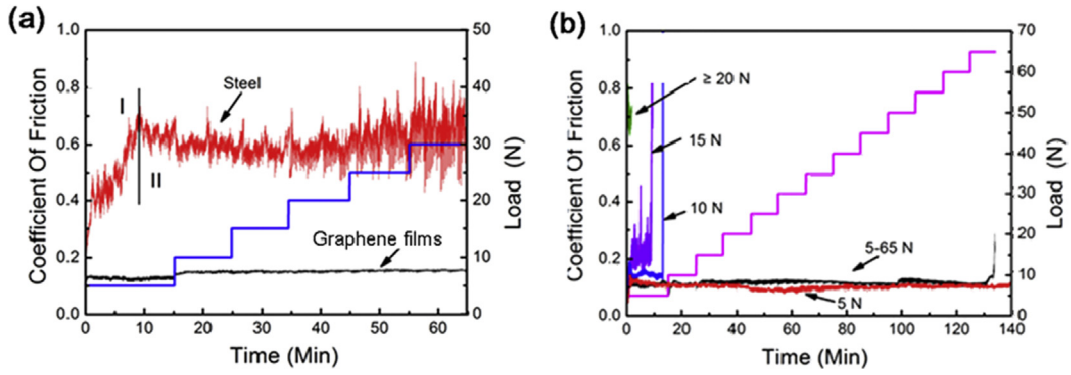

Fig. 3. Friction coefficients of graphene films: (a) under variation loads from 5 to 30N and (b) under loads of 5, 10, 15, 20 N and variation loads 5–65 N.

wavelength of 532 nm (2.3eV)) was applied to reveal the microstructure of the wear surface. The topographies of debris were observed by HRTEM. The friction-load curves were recorded on a multifunctional material surface performance tester (MFT-4000, China), and the wear volumes were obtained by three-dimensional surface profiler (MicroXAM-3D).

3. Results and disscussion

The 201 staless wafers (20 mm × 20 mm) are firstly undergo a wiredrawing processing, and the roughness about 170 nm confirmed by atomic force acoustic microscope (AFM) (Fig. 2a). Then a 2B pencile was reciprocating sliding on steel surface in a direction perpendicular to the wiredrawing grain that easier to grow graphene films. The debris of graphene after rubbing, tested under HRTEM and Raman spectroscope, are shown in Fig. 2b. The graphene films show a fine crystal structure under HRTEM, and which is proved again by Raman spectra that an obvious G peak at 1581 cm^{-1} and a D band at 1349 cm^{-1} can be seen, of which are attributed to in-plane bond stretching of aromatic carbons in the graphitic structure (vibration modes E_{2g}) and breathing mode with A_{1g} symmetry [25–29]. Besides the main peaks, there are five satellite peaks at 1621, 2457, 2689, 2936, and 3247 cm^{-1}. The 1621 cm^{-1} peak, usually reffered as D′ peak, can be observed from defect graphite or graphene, originates from the LO phonons near the Γ point [28–32]. 2457 cm^{-1} band are assigned the band as "$q = 0$" branch of double resonance Raman scattering [33,34], 2689 cm^{-1} band arises from 2D vibration, 2936 cm^{-1} comes from

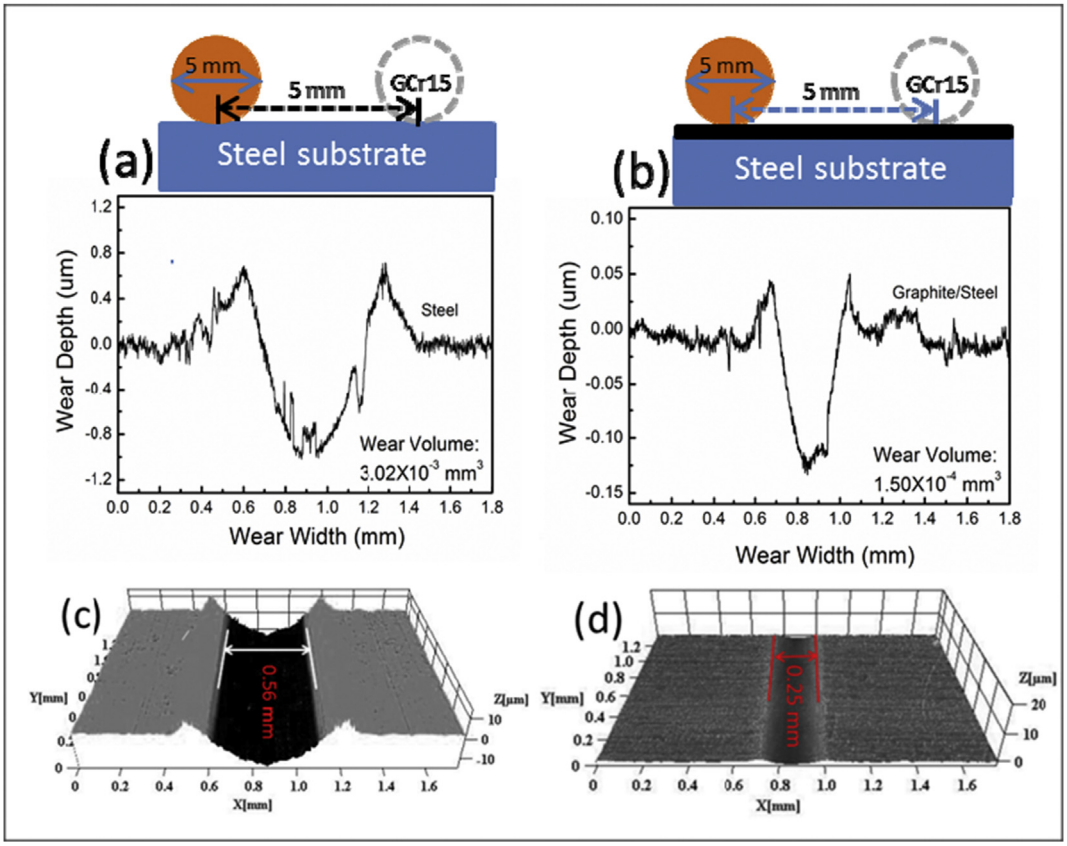

Fig. 4. The 2D cross-section surface profile (top row) and 3D scanning morphologies (bottom) of wear tracks under variable load 5–30 N condition.

D + G(S) vibration which is induced by two TO phonons around the K point and 3247 cm^{-1} peak arises from 2D' [25–34]. At this time we belive that polycrystal are grown on 201 staless wafers.

Then the films were employed to do friction test under a reciprocating friction testing machine. All the friction tests were proceeding in a direction perpendicular to the wiredrawing grain because that the graphene was easier push out of the contant interface in paralled directions. In order to more detailed study of the lubrication mechanism of the CNTs film, here, GCr15 balls ($\Phi = 5$ mm) were employed as the friction pairs. Some of the results are displayed in Fig. 3a. Not surprisingly, graphene films cannot bear the loads beyond 5 N (Fig. 3b). It is easy to see that pencile sketch is limited to densen films, and this will result in the compaction degree of that the films is poor. In this case, if applying a high initial load, the films will wear out soon, and the wear out time is inversely proportional to the initial load (see olive, red, and purple line of Fig. 3b). As we all know, when building a new road, a road roller is usually used to compaction and flattened the road. Inspired by a road roller, thus, in order to obtain the friction data under high loads, and aiming to prolong the life and improve the bearing capacity of the pencil sketch graphene films. Firstly, the graphene films were harding under 5 N loads due to squeezed effects, and then increasing laods step by step to high load under a loading speed of 5 N in every 10 min (see the step line in Fig. 3a and b). In this variable loading process, the friction life of the films has greatly improved, and the ultimate bearing capacity is up to 65 N. In order to survey the effect of load on structure of these films when the load less than 65 N, 0 N, 5 N, 5–15 N, 5–25 N, 5–35 N, 5–45 N and 5–55 N experiments have been done separately. Then, wear traces and debrises were observed via Raman and HRTEM, respectively (discussion later).

Fig. 3a shows the friction curves of steel before and after sketch graphene films under the variable loads (5–30 N) conditions. It is clear that the bare stainless steel friction curve have two regimes, running-in (I) and stable stage (II). In the running-in regime, friction cofficient tends to increase. The reasons may be that rough surface hinder the fully contant with the ball at begining. However, in stable stage the friction cofficient of bare steel substrate against GCr15 ball as high as 0.65, and it remains unstable and fluctuate seriously, especially under the high load, due to the strong adhenssion effects. In contrast, for the graphene/steel, due to the Van der Waals forces between the layers is low, a low and relatively stable friction cofficient (~0.12) could be obtained, and more importantly, the friction cofficient is immune to the change of load. Here, we call such a variable load (from 5 to 65 N) friction process as a steady process (Fig. 3b), and it is essential to mechanical equipment work under the changing-condition for reducing friction and extend the lifespan.

Wear resistance is another important manifestation of the performance of solid films. To better understanding that, both 2D cross-section surface profile (Fig. 4a and b) and 3D scanning morphologies (Fig. 4c and d) of wear tracks under variable loads 5–30 N conditions were measured. On bare steel substrates, the wear track for bare steel substrate up to 0.56 mm and 1.05 μm in width and depth, respectively (Fig. 4a and c), and the wear volume is 3.02×10^{-3} mm^3. In contrast, however, the wear tracks for sketch graphene films is shallower and narrower, about 0.25 mm and 0.13 μm in width and depth, respectively (Fig. 4b and d), and the wear volume is 1.05×10^{-4} mm^3, which only 1/28 of the values of the bare steel substrate. Considering the roughness of steel wafers (170 nm or 0.17 μm, comparable to the wear depth), one can speculate that, with graphene films' protection, the steel has no abrasion but plastic deformation instead. Namely, pencil sketch films could reduce wear of the steel substrate significantly.

Until now, one can confirm that pencil sketch is an effective solid lubricating films preparation method. But we still do not know what happened in nanoscale. People can suppose that if the graphene can be easy exfoliated which afford to the low friction, it can not be sustaining for a long friction life at high load. To reveal that, wear trace and debris were observed via Raman and HRTEM, respectively.

Raman spectroscopy has historically played an important role in the structural characterization of graphitic materials, in particular providing valuable information about defects, stacking of the graphite [35]. Fig. 5 shows the Raman spectra of the as-prepared films as well as the wear traces after friction with different variable loads in the wavelength range of 200–4000 cm^{-1}. Through comparing the Raman spectra under different variable loads, it is obvious of that as-prepared films (0N) there is a D′ peak (1620 cm^{-1}), but disappeared after friction. To further investigate the effect of loads on defects of these films, we employed Gauss fitting to quantitative analysis the I_D/I_G (Fig. 6b) and peak shift move (Inset). After friction test, the relative intensity of the D and G peak weaken significantly due to the thining of graphene films. The value of I_D/I_G decreases with red shift of G peak and blue shift of D peak which indicate that the size of graphene decrease. And the band between 3000 and 3500 cm^{-1} comes widen and tow peaks at 2457, and 3247 cm^{-1} are overlaped or disappeared due to the reinforce of bands at 2689, 2936 cm^{-1} and new peak at 3200 cm^{-1} (Fig. 6). It seems that the bands at 2689, 2936 and 3200 cm^{-1} turn up a strong relationship with the size of graphene (Fig. 6). To further analysis, the bands between 3000 and 3500 cm^{-1} is fitted

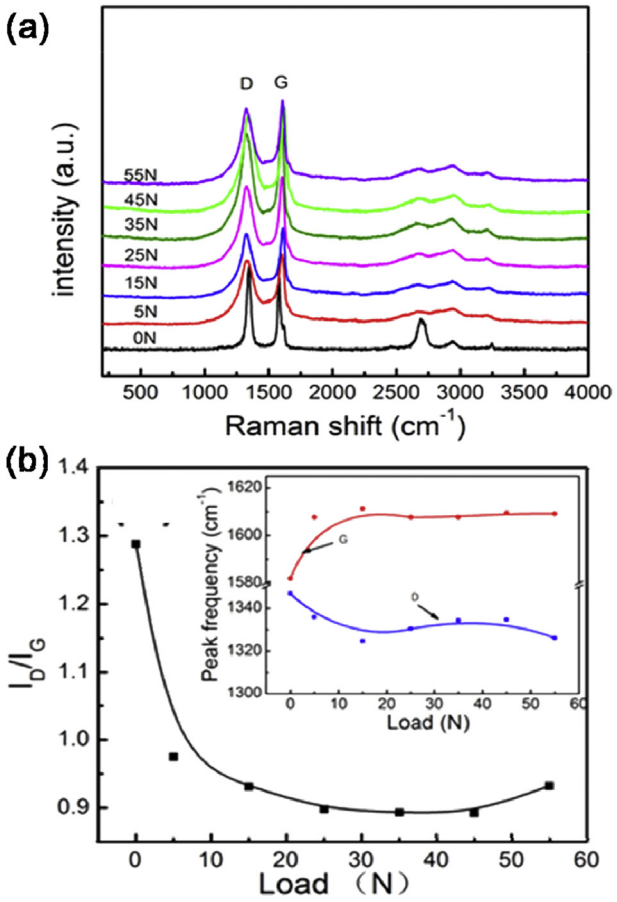

Fig. 5. (a) Raman sectra of graphene film (0N) and friction trace of the graphene films under different loads and (b) ID/IG values as a function of loads and the D and G peak position.

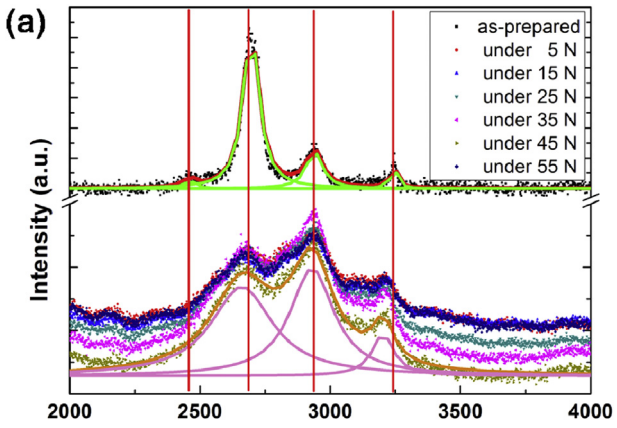

Fig. 6. Raman Spectra of as-prepared graphene films (un one) and of wear traces after friction (down one).

with Lorentzian function. The results show that the peaks relative intensity are unchanged with viration of loads. This results are accordance well with the vary of the I_D/I_G values and D and G peaks position. That is, the microstructure keeps the same beyond the load of 5 N, i.e., after a load desification under 5 N, the graphene films' structure very stabe under different loads friction process.

It is very interesting if one consider the change of friction coefficient that of which keeps constant and steady, and has nothing to do with loads, which is a big difference from friction properties under micro-loads [3]. Kumar et al. Reported that load dependent nonlinear trend of friction coefficient was observed in graphene when tested under ambient atmospheric conditions with ten's of mN load and they stated that friction in grapheneis increases with increase in loads due to lattice disordering [36]. and hexagonal crystal trasition to orthromhombic phase has been confirmed [36]. The increase of friction coefficient has also reported on armorphous carbon films, and is a norm [37–39].

To further reveal the structural evolution during the friction process, HRTEM test was conducted for wear debris and the corresponding images (Fig. 7) show that after friction at 5 N, amorphous structure appears with graphenes (Fig. 7b), incontrast with as-prepared films that only hexagonal grapheneare observed. Even at high load of 55 N, still graphene mixed with amorphous matrix can be seen (Fig. 7c), and the corresponding debris from GCr15 ball show similar hybrid structure with the film of wear trance (Fig. 7d). These results are well agree with the Raman results. When take into account the structure influence, it obviously conclude that our results are closer to neither grahite under micro-loads conditions nor amorphous carbon fims under high loads because that multicrystal graphene films in present work are undergo high loads distinct from the friction test to graphene and are very different from that amorphous carbon fims which has a structure trasition during frition, but not happened in our work. One can confirm that only a desification happen under 5 N in a short friction and there is no obvious change beyond that which can coclude from both HRTEM and Raman results.

Untill now, one can speculate that under short friction, the graphene films structure come to a steady state which can tolerance 65 N reciprocating friction without further structure changing. Combined all resukts together, one can conclude that the shearing force induced the film densification via sp^2 to sp^3 changing that enforce cross-linking under 5 N short friction. This cross-linking carbon matrix was responsible for high load bearing and the graphene exfoliated into graphene under shearing force contribute to low steady-state friction. The reasons why the coefficients not to goes down to lower or super-low friction are that, firstly, the roughness of the steel wafer is non-negligible though after friction it is smoother, and secondly, the presence of amorphous matrix hindered the slipping of graphite. On the other hand, the smooth surface can not hinder the slippage which attribute to the fail of lubricant on steel surface under 65 N.

4. Conclusion

Graphene films for solid lubricating can be obtained by pencil sketch on a stainless steel wafers along the perpendicular to the direction of the texture of the wafer. When applied variable load to the pencil sketch graphene films, which presents low friction, low wear, and the wear tracks are shallow and narrow, the curves of

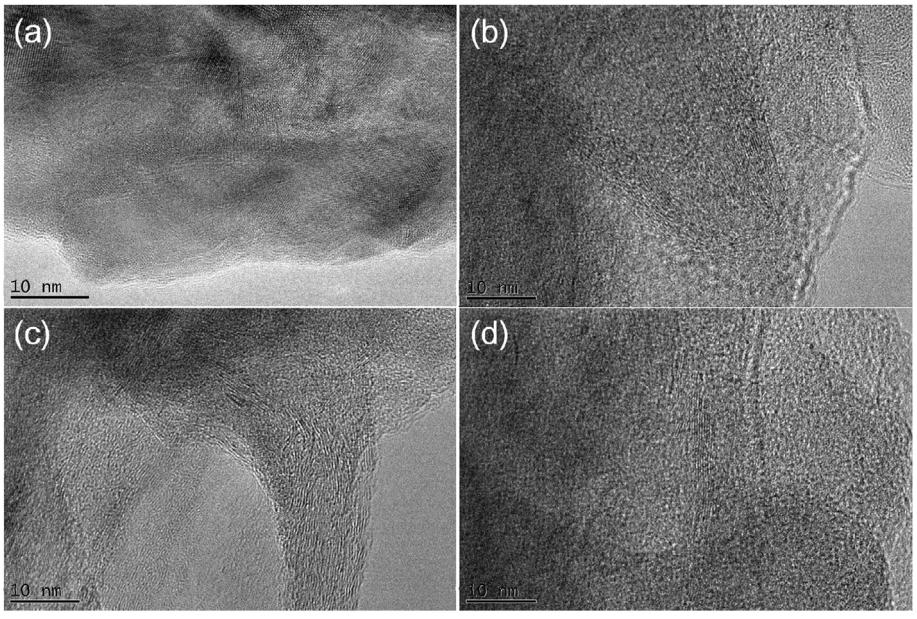

Fig. 7. The FESEM (a) and HRTEM images (a1) of CNTs and FESEM micrograph of CNTs film as-prepared (b).

friction remains stable, moreover, the lifespan and bearing capacity greatly have improved, and the ultimate bearing of graphene films is 65 N. It is commendable that the entire variable loads friction process was a steady-state process. Many of the above phenomena show that the pencil sketch graphene films have good lubricating properties when they used as solid lubricant. Moreover, frictional effect makes the orderliness of the graphene better. Namely, the variable load friction process is a ordering process of the disordered graphite. Benefit from sketch, one can get a lubrication film on any substrates with complex topography, our results shed light on the growth of graphene films for industrial use help understanding the tribology of graphene under high loads.

Acknowledgements

This work was supported by CVS “Light of West China” Program, Youth Innovation Promotion Association CAS (Grant No. 2017459), the China Scholarship Council (Grant No. 201604910183), the Natural Science Foundation of Gansu Province, China (Grant No. 1501RJZA012), and the National Natural Science Foundation of China (Grant No. 51205383, 51611530704 and 51661135022).

References

[1] M. Nosonovsky, B. Bhushan, Theme issue green tribology, Philos. Trans. R. Soc. Lond. Ser. A 368 (1929) (2010) 4755.
[2] M.R. Cai, R.S. Guo, F. Zhou, W.M. Liu, Lubricating a bright future: lubrication contribution of energy saving and low carbon emission, Sci. China Technol. Sci. 56 (12) (2013) 2888.
[3] C.C. Vu, S. Zhang, M. Urbakh, Q. Li, Q.C. He, f Zheng, Thermal induced graphene rotation on hexagonal boron nitride, Phys. Rev. B 94 (2016) 081405(R).
[4] J. Yang, Z. Liu, F. Grey, Z. Xu, X. Li, Y. Liu, M. Urbakh, Y. Cheng, Q. Zheng, Observation of high-speed microscale superlubricity in graphene, Phys. Rev. Lett. 111 (2013) 029902.
[5] D. Berman, A. Erdemir, A.V. Sumant, Graphene: a new emerging lubricant, Mat. Today 17 (1) (2014) 31.
[6] J. Zhang, B. Zhang, Q. Xue, Z. Wang, Dia. Ultra-elastic recovery and low friction of amorphous carbon films produce by a dispersion of multilayer graphene, Diam. Relat. Mater 23 (2012) 5.
[7] S.W. Liu, H.P. Wang, Q. Xu, T.B. Ma, G. Yu, C. Zhang, D. Geng, Z. Yu, S. Zhang, W. Wang, Y.Z. Hu, H. Wang, J. Luo, Robust microscale superlubricity uner high contact pressure enabled bu graphene-coated microsphere, Nat. Commun. 8 (2017) 14029.
[8] Z. Gong, X. Jia, W. Ma, B. Zhang, J. Zhang, Hierarchical structure graphitic-like/MoS 2 film as superlubricity material, Appl. Surf. Sci. 413 (2017) 381.
[9] J. Quereda, A. Castellanos-Gomez, N. Agraït, G. Rubio-Bollinge, Single-layer MoS_2 roughness and sliding friction quenching by interaction with atomically flat substrates, Appl. Phys. Lett. 105 (2014) 053111.
[10] H. Li, J. Wang, S. Gao, Q. Chen, L. Peng, K. Liu, X. Wei, Superlubricity between MoS_2 monolayers, Adv. Mat. 29 (2017) 1701474.
[11] Z. Gong, J. Shi, B. Zhang, J. Zhang, Graphene nano scrolls responding to superlow friction of amorphous carbon, Carbon 116 (2017) 310.
[12] E. Gnecco, E. Meyer, in: S. Cahangirov, S. Ciraci (Eds.), Fundamentals of Friction and Wear on the Nanoscale, Springer, 2015, pp. 463–487.
[13] M. Dienwiebel, G.S. Verhoeven, N. Pradeep, J.W.M. Frenken, J.A. Heimberg, H.W. Zandbergen, Superlubricity of graphite, Phys. Rev. Lett. 92 (2004) 126101.
[14] G.S. Verhoeven, M. Dienwiebel, J.W.M. Frenken, Model calculations of superlubricity of graphite, Phys. Rev. B 70 (2014) 165418.
[15] R. Zacharia, H. Ulbricht, T. Hertel, Interlayer cohesive energy of graphite from thermal desorption of polyaromatic hydrocarbons, Phys. Rev. B 69 (2004) 155406.
[16] J.M. Campanera, G. Savini, I. Suarez-Martinez, M.I. Heggie, Density functional calculations on the intricacies of Moiré patterns on graphite, Phys. Rev. B 75 (2007) 235449.
[17] M. Hasegawa, K. Nishidate, H. Iyetomi, Semiempirical approach to the energetics of interlayer binding in graphite, Phys. Rev. B 76 (2007) 115424.
[18] L. Spanu, S. Sorella, G. Galli, Nature and strength of interlayer binding in graphite, Phys. Rev. Lett. 103 (2009) 196401.
[19] A.M. Popov, I.V. Lebedeva, A.A. Knizhnik, Y.E. Lozovik, B.V. Potapkin, Commensurate-incommensurate phase transition in bilayer graphene, Phys. Rev. B 84 (2011) 045404.
[20] R.H. Savage, Graphite lubrication, J. Appl. Phys. 19 (1948) 1.
[21] P.J. Bryant, P.L. Gutshall, L.H. Taylor, A study of mechanisms of graphite friction and wear, Wear 7 (1964) 118.
[22] N. Kumar, S. Dash, A.K. Tyagi, B. Raj, Super low to high friction of turbostratic graphite under various atmospheric test conditions, Tribol. Int. 44 (2011) 1969.
[23] O. Hod, Interlayer commensurability and superlubricity in rigid layered materials, Phys. Rev. B 86 (2012) 075444.
[24] J. Xiao, L. Zhang, K. Zhou, J. Li, X. Xie, Z. Li, Anisotropic friction behaviour of highly oriented pyrolytic graphite, Crabon 65 (2013) 53.
[25] Y. Sato, M. Kamo, N. Setaka, Raman spectra of carbons at 2600-3300 cm^{-1} region, Carbon 16 (1978) 279.
[26] H. Wang, J.T. Robinson, X. Li, H. Dai, Solvothermal reduction of chemically exfoliated graphene sheets, J. Am. Chem. Soc. 131 (2009) 9910.
[27] M.R. Ammar, J.N. Rouzaud, C.E. Vaudey, N. Toulhoat, N. Moncoffre, Characterization of graphite implanted with chlorine ions using combined Raman microspectrometry and transmission electron microscopy on thin sections prepared by focused ion beam, Carbon 48 (2010) 1244.
[28] C. Casiraghi, A. Ferrari, J. Robertson, Raman spectroscopy of hydrogenated amorphous carbons, Phys. Rev. B 72 (8) (2005) 085401.
[29] C. Castiglioni, F. Negri, M. Rigolio, G. Zerbi, Raman activation in disordered graphites of the A1′ymmetry forbidden $k \neq 0$ phonon: the origin of the D line, J. Chem. Phys. 115 (8) (2001) 3769.
[30] A.C. Ferrari, Raman spectroscopy of graphene and graphite: disorder, electron–phonon coupling, doping and nonadiabatic effects, Solid state Commun. 143 (1) (2007) 47.
[31] F. Tuinstra, J.L. Koenig, Raman spectrum of graphite, J. Chem. Phys. 53 (3) (1970) 1126.
[32] V. Zólyomi, J. Koltai, J. Kürti, Phys. Resonance Raman spectroscopy of graphite and graphene, Status Solidi B 248 (2011) 2428.
[33] T. Shimada, T. Sugai, C. Fantini, M. Souza, L.G. Cançado, A. Jorio, M.A. Pimentab, R. Saito, A. Grüneis, G. Dresselhaus, M.S. Dresselhaus, Y. Ohno, T. Mizutani, H. Shinohara, Origin of the 2450 cm^{-1} Raman bands in HOPG, single-wall and double-wall carbon nanotubes, Carbon 43 (2005) 1049.
[34] E.F. Antunes, A.O. Lobo, E.J. Corat, V.J. Trava-Airoldi, A.A. Martin, C. Veríssimo, Comparative study of first-and second-order Raman spectra of MWCNT at visible and infrared laser excitation, Carbon 44 (2006) 2202.
[35] M. Pimenta, G. Dresselhaus, M.S. Dresselhaus, L.G. Cançado, A. Jorio, R. Saito, Studying disorder in graphite-based systems by Raman spectroscopy, Phys. Chem. Chem. Phys. 9 (2007) 1276.
[36] N. Kumar, A.T. Kozakov, T.R. Ravindran, S. Dash, A.K. Tyagi, Load dependent friction coefficient of crystalline graphite and anomalous behavior of wear dimension, Tribol. Int. 88 (2015) 280.
[37] Z. Wang, C.B. Wang, B. Zhang, J.Y. Zhang, Ultralow friction behaviors of hydrogenated fullerene-like carbon films: effect of normal load and surface tribochemistry, Tribol. Lett. 41 (2011) 607.
[38] Z. Gong, J. Shi, W. Ma, B. Zhang, J. Zhang, Engineering-scale superlubricity of the fingerprint-like carbon films based on high power pulsed plasma enhanced chemical vapor deposition, RSC Adv. 6 (2016) 115092.
[39] Z. Gong, X. Jia, W. Ma, B. Zhang, J. Zhang, Hierarchical structure graphitic-like/MoS 2 film as superlubricity material, Appl. Surf. Sci. 413 (2017) 381.